Polyhedron 43 (2012) 63–70

Contents lists available at SciVerse ScienceDirect

Polyhedron

journal homepage: www.elsevier.com/locate/poly

Heterogeneous catalysis over a barium carboxylate framework compound: Synthesis, X-ray crystal structure and aldol condensation reaction

Debraj Saha, Tanmoy Maity, Rupam Sen [1], Subratanath Koner *

Department of Chemistry, Jadavpur University, Kolkata 700032, India

ARTICLE INFO

Article history:
Received 28 March 2012
Accepted 30 May 2012
Available online 17 June 2012

Keywords:
Hydrothermal synthesis
Alkaline earth metal
Metal–organic framework
Heterogeneous catalysis
Aldol condensation

ABSTRACT

A new three-dimensional alkaline-earth metal–organic framework (MOF) compound, $[Ba(pdc)]_n$ (**1**) (H_2pdc = pyridine-2,5-dicarboxylate), has been hydrothermally synthesized and structurally characterized by single crystal X-ray diffraction analysis. X-ray single-crystal analysis reveals that each metal ion in compound **1** is coordinated by seven O atoms from seven different carboxylate groups. While each pyridine-2,5-dicarboxylato (pdc^{2-}) ligand coordinates to seven alkaline earth metal centers through two carboxylate groups adopting μ_4-η^2:η^2-bridging and μ_3-η^2:η^1-bridging coordination modes to afford a 3D network. Thermogravimetric analysis reveals that compound **1** is thermally stable up to around 560 °C. Compound **1** efficiently catalyzes aldol condensation reactions of various aromatic aldehydes with acetone and cyclohexanone under environment friendly heterogeneous condition, giving remarkable yields (up to 96%) with high selectivity (100%) within a short reaction time (6 h). The catalyst was recycled for five successive runs without significant loss of activity. There was no evidence of leaching of metal ions or no loss of structural integrity of the catalyst during the catalytic reaction.

1. Introduction

Hybrid inorganic–organic compounds are of current interest, not only because of their fascinating variety of architectures and topologies [1], but also owing to their potential applications, particularly in catalysis [2,3], molecule-based magnetic materials [4–6], artificial nucleases for the hydrolytic cleavage of DNA and RNA [7], contrast agents for magnetic resonance imaging [8] and fixation media for atmospheric gases [9]. In such materials, functionality can be introduced from either the inorganic species or the organic linkers. Multidimensional M–O–M frameworks have demonstrated cooperative effects which can also lead to improved thermal stabilities [10]. Metal carboxylates are particularly interesting because they exhibit open-framework structures and the carboxylate group acts as a linker between inorganic moieties [11]. Metal dicarboxylates have a wide range of application in the construction of coordination polymer arrays, especially with the more rigid ligands, as they act as building blocks for porous networks with various metal ions [12]. Pyridine dicarboxylic acid (H_2pdc) seems to be a potential rigid ligand in building metal–organic framework compounds (MOFs). The O- and N-donor sites of H_2pdc allow it to produce different types of interesting 3D structures consisting of transition metal and lanthanide ions [13–15]. In comparison to other pyridine dicarboxylic acids, H_2pdc seems to easily coordinate to metal ions to form an infinite structure, because the two carboxylate groups on the opposite sides of the aromatic moiety may give rise to more stability in MOF structures.

There have been quite a few studies [16] on the coordination behavior of alkaline earth metals in both aqueous and non-aqueous media. Barium based MOFs containing the organic linker 2,5-pyridinedicarboxlic acid have been reported [17,18]. Fromm has recently reviewed coordination polymer networks with s-block metal ions [16]. Two reasons prevent the use of s-blocks in the metal–organic frameworks design, *viz.* their unpredictable coordination numbers and geometries as no ligand field stabilization effects govern their coordinate bonding, and their tendency to form solvated metal centers, and thus, the formation of the typical alternating $[M(H_2O)_6]L$ (M = alkaline-earth metal, L = ligand) organic–inorganic ionic layers [19]. Besides, lack of intrinsically useful properties (i.e. magnetism or variable oxidation states) might appear to make alkaline earth metals less interesting. Nevertheless these metals have some advantages for the application in materials science; they are non-toxic, cheap and generally soluble in aqueous preparation. For these reasons alkaline earth salts are the preferred formulation for a host of commercial materials, including many common pharmaceuticals, dyes and pigments [16]. In this context some recent studies concerning alkaline-earth metal complexes deserve to be mentioned [20–23]. Platero-Prats et al. studied alkene hydrogenations and ketone hydrosilylation reactions over alkaline-earth

---

* Corresponding author. Tel.: +91 33 2457 2778; fax: +91 33 2414 6414.
E-mail address: snkoner@chemistry.jdvu.ac.in (S. Koner).

[1] Present address: Department of Chemistry, CICECO, University of Aveiro, 3810-193 Aveiro, Portugal.

0277-5387/$ - see front matter © 2012 Elsevier Ltd. All rights reserved.
http://dx.doi.org/10.1016/j.poly.2012.05.043

sulfonate metal–organic frameworks, which show 100% selectivity towards ethylbenzene under homogeneous conditions [24]. Hydrogenation of styrene catalyzed by a Ca based MOF has also been studied under heterogeneous conditions [25]. Choudary et al. studied aldol-condensation reactions over nanocrystalline magnesium oxide, which showed higher activity in direct asymmetric aldol-condensation reactions under heterogeneous conditions [26]. Baruah et al. studied aldol-condensation reactions catalyzed by magnesium carboxylate compounds under homogeneous conditions [27]. Homogeneous catalysts, however, suffer from the problems of recycling of the catalyst as the separation of the catalyst from the reaction mixture is troublesome. Recycling of a catalyst is a task of great economic and environmental advantage in chemical and pharmaceutical industries.

In the course of our continuing investigation on the catalytic uses of MOFs we have successfully used layered metal carboxylates and lanthanide-based MOFs to catalyze olefin epoxidation reactions under heterogeneous condition [28–31]. Further exploration of alkaline-earth metal based MOFs afforded a new 3D MOF involving barium and pyridine-2,5-dicarboxylic acid [H_2pdc], $[Ba(pdc)]_n$ (**1**). Interestingly, compound **1** features a 3D framework structure and efficiently catalyzes the aldol-condensation reactions under heterogeneous condition. Compound **1** is a rare example of a barium based framework compound which is capable of catalyzing aldol condensation reactions under heterogeneous condition.

2. Experimental

2.1. Materials and physical measurements

Barium nitrate, pyridine-2,5-dicarboxylic acid and the substituted benzaldehydes were purchased from Aldrich and were used as received. Other chemicals were purchased from Merck (India). Benzaldehyde, acetone and tetrahydrofuran were distilled before use. Benzaldehyde was kept over NaA molecular sieves to trap possible traces of benzoic acid. Elemental analyses were performed using a Perkin–Elmer 240C elemental analyzer. Fourier transformed infrared spectra of samples in KBr pellets were measured on a Perkin–Elmer RX I FT-IR spectrometer. Powder X-ray diffraction (XRD) patterns of the samples were recorded with a Scintag XDS-2000 diffractometer using Cu Kα radiation. TG analysis was performed on a Perkin–Elmer (SINGAPORE) Pyris Diamond TGA unit. The heating rate was programmed at 5 °C min^{-1} with a protecting stream of N_2 flowing at a rate of 150 ml min^{-1}. N_2 sorption measurements were performed on an Autosorb iQ (Quantachorme Inc., USA) gas sorption system at 77 K. The sample was degassed at 100 °C for 3 h under vacuum (10^{-3} Torr) prior to nitrogen sorption measurements.

2.2. Synthesis of the compound

Compound **1** was synthesized through a hydrothermal route. The compound was obtained as colorless block crystals after heating in a 25 ml Teflon-lined Parr acid digestion bomb at 150 °C for 3 days, followed by slow cooling at a rate of 5 °C/h to room temperature. The initial reaction mixture was prepared by mixing barium nitrate (0.522 g, 2 mmol) and pyridine-2,5-dicarboxylic acid (0.167 g, 1 mmol) in 8 ml of milliQ water. The pH of the reaction mixture was adjusted to 8 by adding dilute NaOH solution. The crystals obtained were filtered off by suction and washed several times with distilled water and then with acetone to remove impurities, and finally dried in air. The bulk compound was characterized by elemental analysis and an IR spectroscopic study. For $[Ba(Pdc)]_n$ (**1**). Selected IR peaks (KBr disk, ν, cm^{-1}): 1607, 1685 [ν_{as} (CO_2^-)], 1390 [ν_s(CO_2^-)], 1366, 1177 [ν_s (C–O)]. *Anal.* Calc. C, 27.80; H, 0.99; N, 4.63. Found: C, 27.8; H, 1.0; N, 4.5%.

2.3. X-ray crystallography

X-ray diffraction data of **1** were collected at 293(2) K on a Bruker SMART APEX CCD X-ray diffractometer using graphite-monochromated Mo Kα radiation (λ = 0.71073 Å). Integrated intensities were determined and the unit cell was refined with the SAINT [32] software package using a narrow-frame integration algorithm. An empirical absorption correction (SADABS) [33] was applied. The structure was solved by direct methods and refined against F^2 using the full-matrix least-squares technique with anisotropic displacement parameters for non-hydrogen atoms with the programs SHELXS97 and SHELXL97 [34]. The carbon bound hydrogen atoms were freely refined. There were no remarkable peaks in the final difference Fourier maps, except for ghost peaks surrounding the metal center.

2.3.1. X-ray crystallography data of $[Ba(pdc)]_n$ (1)

$C_7H_3NO_4Ba$, M = 302.43, orthorhombic, space group *Pbca*, a (Å) = 7.762(10), b (Å) = 10.506(2), c (Å) = 18.3021(4), V ($Å^3$) = 1492.69(5), Z = 8, R_{int} = 0.0322, D_{calc} (g/cm^{-3}) = 2.692, F(000) = 1120, μ (mm^{-1}) = 5.296, $\Delta\rho_{max}$ (e $Å^{-3}$) = 0.874, $\Delta\rho_{min}$ (e $Å^{-3}$) = −0.979, Goodness-of-fit (GOF) on F^2 = 1.270, T = 293(2).

2.5. Catalytic reactions

The catalytic reactions were carried out in a glass batch reactor according to the following procedure. Acetone/cyclohexanone (10 mmol), triethylamine (2 mmol), tetrahydrofuran (2 ml) and the catalyst (5 mg) were placed in a round-bottom flask. The flask was then placed in an ice-bath, maintaining the temperature 5–10 °C. The desired aldehyde (2 mmol) was then added to the solution and the reaction mixture was stirred for 6 h (Scheme 1). After the reaction, the catalyst was separated by filtration and the product was purified by column chromatography on silica gel (60–120 mesh), eluting with *n*-hexane/ethyl acetate. The product was analyzed by ^{1}H NMR spectroscopy and elemental analysis, and the data were compared with those of authentic samples.

3. Results and discussion

3.1. X-ray structure of $[Ba(pdc)]_n$ (1)

A single-crystal X-ray crystallographic study reveals that compound **1** crystallizes in the space group *Pbca* with Z = 8. The coordination geometry of the central metal atom in compound **1** is a distorted pentagonal bipyramid. Selected bond distances and angles are collated in Table 1. An ORTEP diagram of **1** with the atom numbering scheme is shown in Fig. S1 (see Supplementary material). In this compound each metal ion is coordinated by seven O atoms from seven different carboxylate groups (Fig. 1a). The Ba–O (carboxylate) bond distances range from 2.710(3) to 2.878(3) Å, which are in agreement with the Ba–O bond lengths observed in other alkaline earth metal carboxylate complexes [16]. Additionally, there are two weak coordinations from carboxylate oxygen and pyridine nitrogen atoms with longer Ba1–O4$^{\#3}$ (#3: $-x$, $-1/2+y$, $3/2-z$) and Ba1–N1$^{\#4}$ (#4: $-x$, $2-y$, $1-z$) bond lengths of 3.010(3) and 3.117(3) Å, respectively [35]. All the carboxylate oxygen atoms in compound **1** are doubly bridged, taking the weaker Ba1–O4 bond into account (Fig. 1). Each pdc^{2-} ligand coordinates to seven alkaline earth metal centers through the carboxylato oxygen atoms, adopting fascinating μ_4-η^2:η^2-bridging and μ_3-η^2:η^1-bridging coordination modes to afford a 3D network

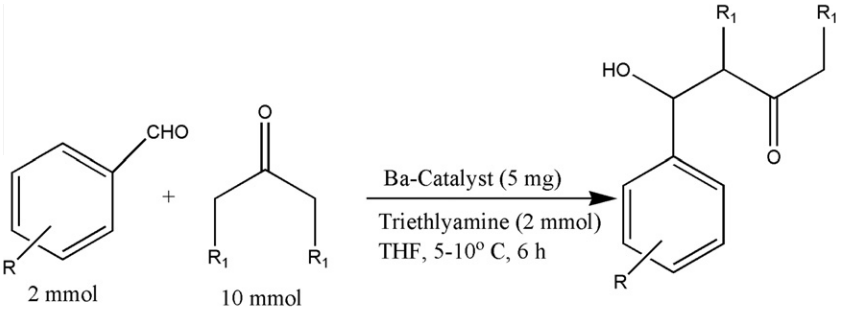

Scheme 1. Aldol condensation reaction catalyzed by compound 1.

Table 1
Selected bond lengths (Å) and angles (°) for the compound **1**.

Bond lengths		Bond angles	
Ba1–O1	2.721(3)	O1–Ba1–O4$^{\#1}$	72.54(8)
Ba1–O4$^{\#1}$	2.825(3)	O1–Ba1–O1$^{\#2}$	137.82(8)
Ba1–O1$^{\#2}$	2.762(2)	O1–Ba1–O5$^{\#3}$	97.03(8)
Ba1–O4$^{\#3}$	3.010(3)	O1–Ba1–O2$^{\#4}$	72.41(9)
Ba1–O5$^{\#3}$	2.878(3)	O1–Ba1–O2$^{\#5}$	73.46(9)
Ba1–O2$^{\#4}$	2.710(3)	O1–Ba1–O5$^{\#6}$	147.00(9)
Ba1–N1$^{\#4}$	3.117(3)	O4$^{\#1}$–Ba1–O5$^{\#3}$	136.41(9)
Ba1–O2$^{\#5}$	2.780(3)	O1$^{\#2}$–Ba1–O4$^{\#1}$	143.11(8)
Ba1–O5$^{\#6}$	2.711(3)	O2$^{\#5}$–Ba1–O4$^{\#1}$	67.66(9)
		O2$^{\#4}$–Ba1–O4$^{\#1}$	107.83(9)
		O4$^{\#1}$–Ba1–O5$^{\#6}$	93.28(9)
		O1$^{\#2}$–Ba1–O5$^{\#3}$	70.80(8)
		O1$^{\#2}$–Ba1–O2$^{\#4}$	73.91(9)
		O1$^{\#2}$–Ba1–O2$^{\#5}$	131.42(9)
		O1$^{\#2}$–Ba1–O5$^{\#6}$	69.43(9)
		O2$^{\#5}$–Ba1–O5$^{\#3}$	108.79(9)
		O2$^{\#7}$–Ba1–O5$^{\#3}$	68.80(9)
		O5$^{\#3}$–Ba1–O5$^{\#6}$	72.53(8)
		O2$^{\#4}$–Ba1–O2$^{\#5}$	145.17(9)
		O2$^{\#4}$–Ba1–O5$^{\#6}$	140.49(9)
		O2$^{\#5}$–Ba1–O5$^{\#6}$	73.58(9)

Symmetry codes: #1: 1/2 – *x*, 2 – *y*, –1/2 + *z*; #2: –1/2 + *x*, 3/2 – *y*, 1 – *z*; #3: –*x*, –1/2 + *y*, 3/2 – *z*; #4: –*x*, 2 – *y*, 1 – *z*; #5: 1/2 – *x*, –1/2 + *y*, *z*; #6: *x*, 3/2 – *y*, –1/2 + *z*.

compound. Ba1 and its symmetry related congeners form one-dimensional zig-zag chains through edge sharing of their coordination polyhedra. The 1D chains are further connected to each other by the edge sharing of the Ba1 polyhedron to afford two-dimensional layers. The interlayer separation was measured to be about 5.75 Å. Further, a dicarboxylate ligand bridges the 2D layers to generate a three-dimensional framework structure (Fig. 2).

3.2. Thermogravimetric analysis

Thermogravimetric analysis of **1** was performed using a powdered sample under a nitrogen atmosphere. TG measurement confirmed that compound **1** is thermally stable up to approximately 560 °C, indicating good thermal stability of this MOF compound (see Supplementary material Fig. S2). The TG curve indicates that compound **1** starts to decompose at approximately 560 °C and completes decomposition at around 700 °C. There are only a few MOF compounds that are reported to be thermally stable above 500 °C [36,37]. The thermal stability of MOFs is usually explained in terms of the rigidity of the linkers, absence of solvent molecules in the network of the MOFs, strong bonds between the metal ions and the organic linkers, etc. Compound **1** satisfies all these requirements.

3.3. Nitrogen sorption study

The nitrogen sorption measurement was undertaken to verify the porous nature of compound **1** as well as to calculate the surface area of the framework. The BET (Brunauer–Emmett–Teller) [38] surface area of **1** was calculated from the N_2 adsorption isotherm. The adsorption and desorption isotherms of **1** are shown in Fig. 3. The adsorption of N_2 follows a type II isotherm, and indicates a

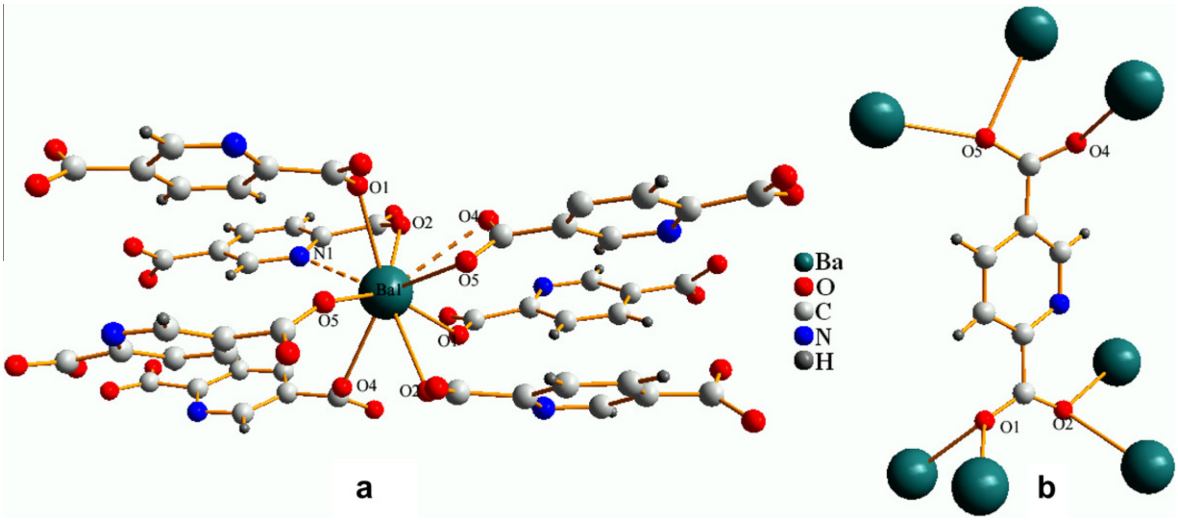

Fig. 1. A segment of compound **1**, showing the local coordination environment of the barium(II) ion (yellow dotted lines for weak interaction) (a); coordination mode of the pdc^{2-} ligand in compound **1** (b). (Color online.)

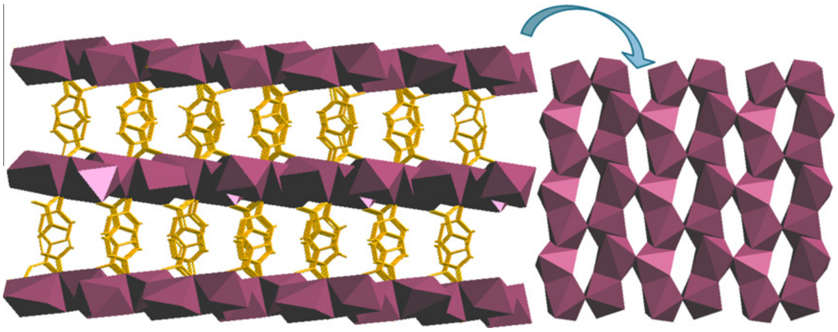

Fig. 2. 3D framework of compound **1**.

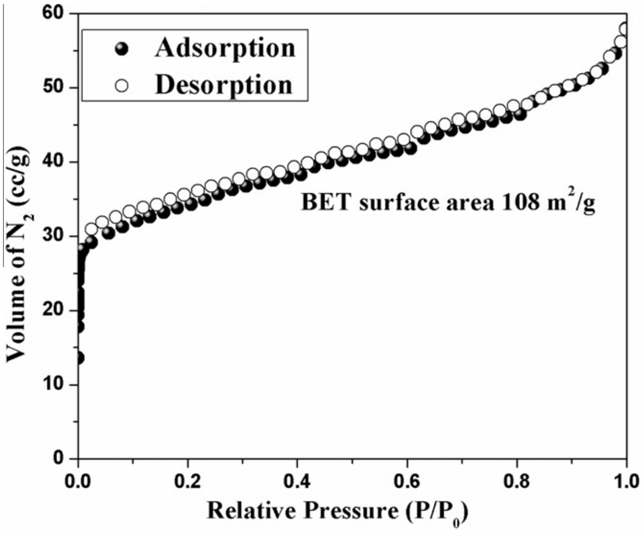

Fig. 3. Plot of the N_2 adsorption–desorption isotherm of compound **1** at 77 K.

surface area (S_{BET}) of 108 m^2 g^{-1} ($S_{Langmuir}$ = 218 m^2 g^{-1}). [Ba(pdc)]$_n$ (**1**) has a very densely packed structure, which is supported by the PLATON [39] calculations. Dense packing can be easily seen in a space filling representation of the structure of **1**. Careful examination of the crystal structure ensures that there are no pores or cavities of appreciable size in compound **1**. [Ba(pdc)]$_n$ (**1**) does not contain either guest or coordinated solvent molecules which could give rise to empty voids in the network after thermal activation. Further, the value of the surface area is low in comparison to that of microporous metal–organic frameworks. The surface area calculated from the N_2 sorption measurement is, therefore, presumably coming mainly from the external surface of the powdered MOF compound.

3.4. Catalytic aldol condensation reaction

Environmental friendly heterogeneous catalytic processes are attracting increased attention in chemical industries. The identification of highly active solid Brønsted-type basic catalysts capable of performing C–C bond formation remains a challenge. The main drawbacks of using NaOH or KOH as homogeneous catalysts are corrosion problems in the equipment, separation difficulties and generation of large amounts of waste. To overcome these disadvantages, several efforts have been made to design new catalytic systems with controlled basic properties in order to increase the efficiency of the process. Among the various magnesium compounds which are used as mediators or catalysts for several organic reactions [40], magnesium oxide is a versatile catalyst for C–C bond formation reactions [41]. Magnesium oxide nano-particles have also been studied for their efficacy in catalyzing aldol condensation reactions [26]. Magnesium carboxylate compounds have attracted little attention with regards to C–C bond formation reactions due to their limited synthetic accessibility and hygroscopic nature [27]. Recently barium containing compounds have been used to catalyze C–C bond formation reactions [42–46] and some of them catalyze aldol condensation reactions [45,46]. We report here the catalytic activity of compound **1** in aldol condensation reactions under heterogeneous conditions (Scheme 1).

The catalytic reactions were performed with a large excess of ketone to prevent self-condensation and to effectively use the aldehyde [47]. During the catalytic reactions, the temperature of the reaction medium was maintained in the range 5–10 °C. On increasing the reaction temperature, benzylideneketone (the condensed product) was obtained from the β-aldol. The reactions were performed in THF medium in the presence of triethylamine, and the results obtained in the reactions are shown in Table 2. The catalytic reactions were also performed in a THF–water medium and under solvent-less conditions using *p*-nitrobenzaldehyde. The best result was obtained in THF medium (Table 3). In THF medium, as well as in solvent-less conditions, the aldehydes were converted to their respective β-aldols as the sole product. We noticed that the β-aldol products did not undergo further transformation to form unsaturated carbonyl compounds, which has been generally observed in previous studies [48,49]. The efficiency of the catalyst followed the order: THF > THF–water > solvent-less condition. No conversion was observed in the absence of catalyst. The catalytic reactions also did not occur in the absence of base (i.e. triethylamine). The yield of the β-aldol product decreased in the sequence *p*- > *o*- > *m*-nitrobenzaldehyde. A nitro substituent at the *ortho* and *para* position may give rise to both a negative inductive effect and a negative mesomeric effect, thereby increasing the electrophilicity of the C=O groups of these nitrobenzaldehydes, whereas substitution at the *meta* position affords only the negative inductive effect. Between *p*-nitrobenzaldehyde and *o*-nitrobenzaldehyde, more steric crowding at the *ortho* position may leads to a low conversion for the *ortho* variety. Additionally, the presence of an electron donating group in the ring, for example *p*-methoxy-benzaldehyde, decreases the yield further and demonstrates the lowest conversion. In case of cyclohexanone a similar trend in the yield of the β-aldol products was observed. Turn over frequencies (TOF) of the aldol reactions catalyzed by [Ba(pdc)]$_n$ (**1**) are given in Table 2. Shibasaki et al. studied similar aldol condensation reactions over a barium catalyst under homogeneous conditions, which showed impressive conversion (up to 99%), however the turnover frequencies of these reactions were very low (0.32–1 h^{-1}) [50]. Aldol condensation reactions catalyzed by magnesium carboxylate under homogeneous conditions also demonstrate lower TOF values (2–5 h^{-1}) than that of compound **1** [27].

Table 2
Reactions of various aromatic aldehydes and acetone/cyclohexanone catalyzed by compound **1**.[a]

Entry	Ketone	Aldehyde	Major product	Isolated yield (wt.%)	TOF[c] (h^{-1})
1	Acetone	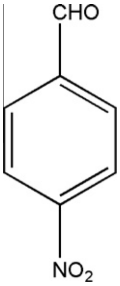	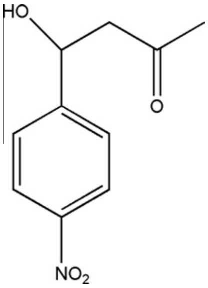	96, 94[b]	19, 19[b]
2	Acetone	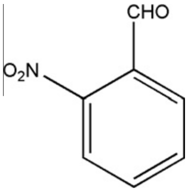	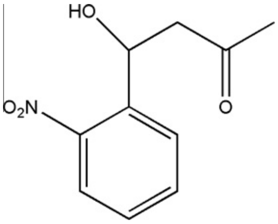	88	18
3	Acetone	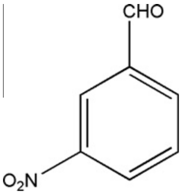	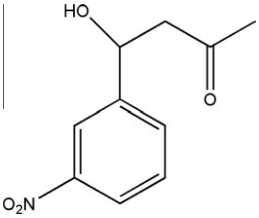	82	16
4	Acetone	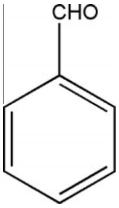	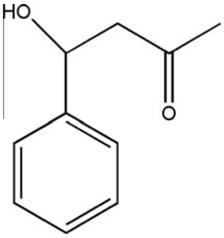	70	14
5	Acetone	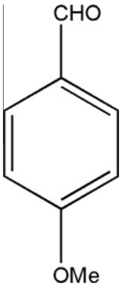	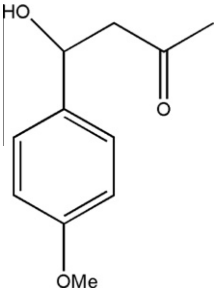	62	12
6	Cyclohexanone	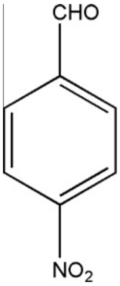	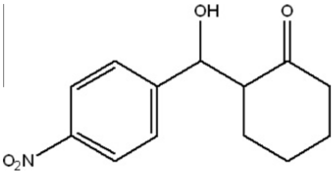	90, 87[b]	18, 17[b]

(*continued on next page*)

Table 2 (*continued*)

Entry	Ketone	Aldehyde	Major product	Isolated yield (wt.%)	TOF[c] (h^{-1})
7	Cyclohexanone	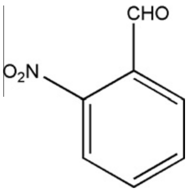	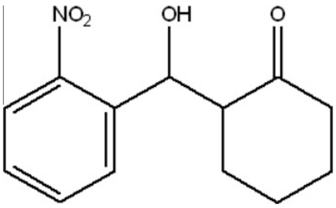	80	16
8	Cyclohexanone	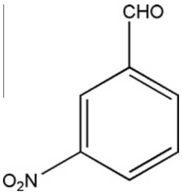	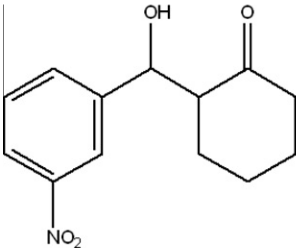	74	15
9	Cyclohexanone	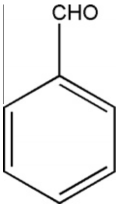	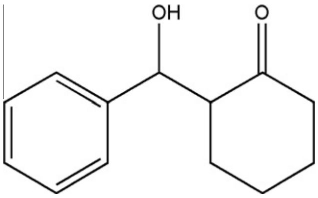	62	12
10	Cyclohexanone	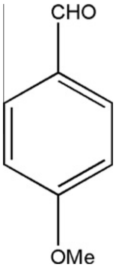	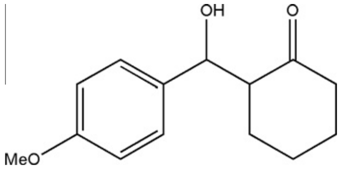	55	11

[a] Reaction conditions: aldehyde (2 mmol), acetone/cyclohexanone (10 mmol), triethylamine (2 mmol), solvent (2 ml) and catalysts (5 mg); temperature = 5–10 °C. Yields were isolated after 6 h of reaction.

[b] Fifth cycle.

[c] Turn over frequency (TOF) = moles converted per moles of active site per unit time.

Table 3
Solvent effect on the aldol condensation of *p*-nitrobenzaldehyde and acetone/cyclohexanone catalyzed by **1**.[a]

Solvent	Ketone	Major product	Isolated yield (wt.%)	Selectivity (wt.%)
THF	Acetone	*β*-Aldol product	96	100
THF	Cyclohexanone	*β*-Aldol product	90	100
THF–water (1:1)	Acetone	*β*-Aldol product	64	62
THF–water (1:1)	Cyclohexanone	*β*-Aldol product	58	60
No solvent	Acetone	*β*-Aldol product	32	100
No solvent	Cyclohexanone	*β*-Aldol product	28	100

[a] Reaction conditions are the same as those given in the footnote of Table 2.

3.4.1. Separation, catalyst reuse and heterogeneity test

To ascertain that the catalysis was indeed heterogeneous, we performed a hot filtration test. The solid catalyst was filtered off when the catalytic reaction was 30–40% complete and the liquid phase of the reaction mixture was kept under the reaction conditions for a further 8 h. Analysis of the products of the catalytic reaction confirmed that there was no further increase of the product. No reaction occurred in the absence of the solid catalyst. This result suggests that there is no leaching of Ba from the solid catalyst during reactions.

To check the stability of the catalyst, we characterized the recovered material. After completion of a catalytic reaction, the solid catalyst was recovered by centrifugation, washed thoroughly with dichloromethane, and dried. The recovered catalyst was then subjected to X-ray powder diffraction analysis and IR spectral analysis. A comparison of the IR spectra (Fig. 4) and X-ray diffraction patterns (Fig. 5) of the pristine compound and recovered catalyst convincingly demonstrates that the structural integrity of the compound is retained after the aldol condensation reaction.

For the recycling study, the aldol condensation reaction was performed using *p*-nitrobenzaldehyde with acetone and cyclohexanone. After the first cycle of the reaction, the catalyst was recovered by centrifugation and then washed as mentioned above. The recovered catalyst was dried under vacuum (~100 °C, 12 h) prior

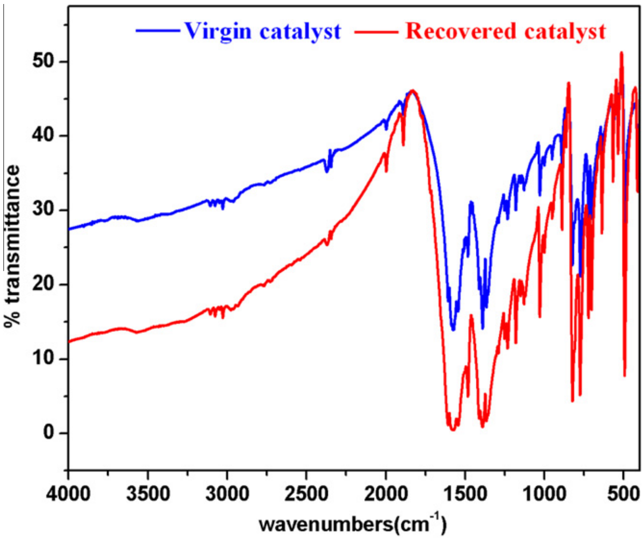

Fig. 4. Comparison of the IR spectra of pure and recovered catalyst for **1**.

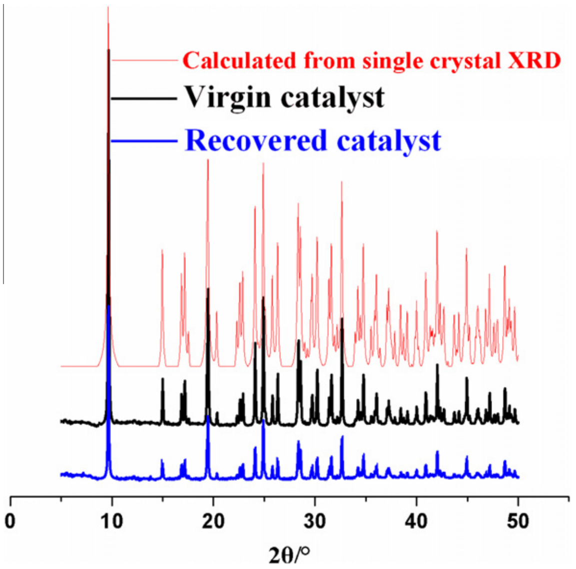

Fig. 5. X-ray powder pattern of the virgin catalyst and recovered catalyst for **1**.

to reuse as a catalyst. The performance of the recycled catalyst after five successive runs is given in Table 2. The catalytic efficacy of the recovered catalyst remained almost the same in each run (Fig. 6).

4. Conclusion

In essence, we have synthesized a new MOF compound, $[\mathrm{Ba(pdc)}]_n$ (**1**), through a hydrothermal route, and this compound is thermally stable up to around 560 °C. $[\mathrm{Ba(pdc)}]_n$ (**1**) displays excellent catalytic activity in aldol condensation reactions of various aromatic aldehydes, giving remarkable yields with high selectivity within a short reaction time under heterogeneous condition. Evidently, the advantage of our system is that the catalyst is not air or moisture sensitive; hence, there is no need to carry out the reaction under an inert atmosphere. The catalyst can be recycled and reused several times without any loss of activity. Our future work will be focused on constructing alkaline-earth metal based frameworks for higher catalytic activity in aldol condensation reactions.

Acknowledgments

We acknowledge the Department of Science and Technology (DST), Government of India for funding a project (to S.K.) (SR/S1/IC-01/2009). We also thank DST for funding the Department of Chemistry, Jadavpur University to procure a single crystal X-ray facility under the DST-FIST program. Financial assistance from UGC under the CAS program is also gratefully acknowledged.

Appendix A. Supplementary data

CCDC 835092 contains the supplementary crystallographic data for **1**. These data can be obtained free of charge via http://www.ccdc.cam.ac.uk/conts/retrieving.html, or from the Cambridge Crystallographic Data Centre, 12 Union Road, Cambridge CB2 1EZ, UK; fax: (+44) 1223-336-033; or e-mail: deposit@ccdc.cam.ac.uk. ORTEP diagram of **1** (Fig. S1), TG analysis curve (Fig. S2), ^{1}H NMR of all products of known compounds and elemental analysis data of the isolated products. Supplementary data associated with this article can be found, in the online version, at http://dx.doi.org/10.1016/j.poly.2012.05.043.

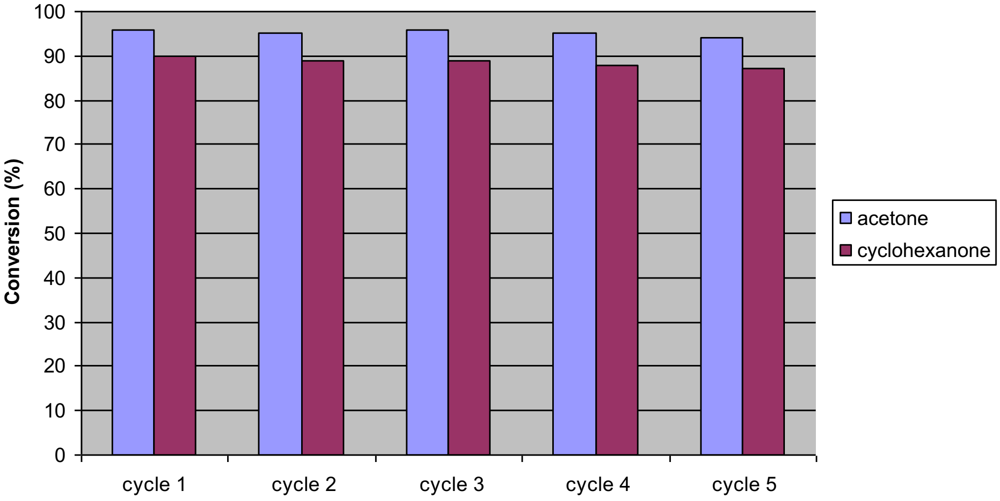

Fig. 6. Aldol condensation of *p*-nitrobenzaldehyde and ketones catalyzed by **1** in five successive runs.

References

[1] Y. Takashima, S. Furukawa, S. Kitagawa, CrystEngComm 13 (2011) 3360.
[2] F. Gándara, E.G. Puebla, M. Iglesias, D.M. Proserpio, N. Snejko, M.A. Monge, Chem. Mater. 21 (2009) 655.
[3] R. Sen, D. Saha, S. Koner, Chem. Eur. J. 18 (2012) 5979.
[4] P.J. Saines, B.C. Melot, R. Seshadri, A.K. Cheetham, Chem. Eur. J. 16 (2010) 7579.
[5] R. Sen, A. Bhattacharya, D. Mal, A. Bhattacharjee, P. Gütlich, A.K. Mukherjee, M. Solzi, C. Pernechele, S. Koner, Polyhedron 29 (2010) 2762.
[6] A. Bhattacharjee, Y. Miyazaki, Y. Nakazawa, S. Koner, S. Iijima, M. Sorai, Physica B 305 (2001) 56.
[7] K. Nwe, C.M. Andolina, C.-H. Huang, J.R. Morrow, Bioconjug. Chem. 20 (2009) 1375.
[8] C.-H. Huang, J.R. Morrow, Inorg. Chem. 48 (2009) 7237.
[9] J. Luo, H. Xu, Y. Liu, Y. Zhao, L.L. Daemen, C. Brown, T.V. Timofeeva, S. Ma, H.-C. Zhou, J. Am. Chem. Soc. 130 (2008) 9626. and references therein.
[10] N. Guillou, P.M. Gao, P.M. Forster, J.S. Chang, S.E. Park, G. Férey, A.K. Cheetham, Angew. Chem. 113 (2001) 2913;
Angew. Chem., Int. Ed. 40 (2001) 2831
[11] M. Eddaoudi, J. Kim, N. Rosi, D. Vodak, J. Wacher, M. O'Keeffe, O.M. Yaghi, Science 295 (2002) 469.
[12] J.L.C. Rowsell, O.M. Yaghi, Angew. Chem., Int. Ed. 44 (2005) 4670.
[13] S.K. Ghosh, P.K. Bharadwaj, Inorg. Chem. 44 (2005) 3156.
[14] X.M. Zhang, Y.Z. Zheng, C.R. Li, W.X. Zhang, X.M. Chen, Cryst. Growth Des. 7 (2007) 980.
[15] P. Mahata, S. Natarajan, Inorg. Chem. 46 (2007) 1250.
[16] K.M. Fromm, Coord. Chem. Rev. 252 (2008) 856.
[17] M.L. Foo, S. Horikes, S. Kitagawa, Inorg. Chem. 50 (2011) (1855) 11853.
[18] Y.-C. Gao, Q.-H. Liu, F.-W. Zhang, G. Li, W.-Y. Wang, H.-J. Lu, Polyhedron 30 (2011) 1.
[19] D.E. Fenton, in: S. Wilkinson, R.D. Gillard, J.A. McCleverty (Eds.), Comprehensive Coordination Chemistry, vol. 3, Pergamon, Oxford, 1987, p. 1.
[20] W.D. Buchanan, E.D. Nagle, K. Ruhlandt-Senge, Main Group Chem. 8 (2009) 263.
[21] J. Langer, S. Krieck, H. Gorls, G. Kreisel, W. Seidel, M. Westerhausen, New J. Chem. 34 (2010) 1667.
[22] S. Krieck, H. Gorls, L. Yu, M. Reiher, M. Westerhausen, J. Am. Chem. Soc. 131 (2009) 2977.
[23] J. Spielmann, D.F.J. Piesik, S. Harder, Chem. Eur. J. 16 (2010) 8307.
[24] A.E. Platero-Prats, M. Iglesias, N. Snejko, Á. Monge, E. Gutiérrez-Puebla, Cryst. Growth Des. 11 (2011) 1750.
[25] A.E. Platero-Prats, V.A. de la Peña-ÓShea, M. Iglesias, N. Snejko, Á. Monge, E. Gutiérrez-Puebla, Cryst. Growth Des. 2 (2010) 147.
[26] B.M. Choudary, L. Chakrapani, T. Ramani, K.V. Kumar, M.L. Kantam, Tetrahedron 62 (2006) 9571.
[27] B.K. Dey, A. Karmakar, J.B. Baruah, J. Mol. Catal. A 303 (2009) 137.
[28] R. Sen, R. Bera, A. Bhattacharjee, P. Gütlich, S. Ghosh, A.K. Mukherjee, S. Koner, Langmuir 24 (2008) 5970.
[29] R. Sen, D.K. Hazra, S. Koner, M. Helliwell, M. Mukherjee, A. Bhattacharjee, Polyhedron 29 (2010) 3183.
[30] R. Sen, S. Koner, D.K. Hazra, M. Helliwell, M. Mukherjee, Eur. J. Inorg. Chem. (2011) 241.
[31] R. Sen, D.K. Hazra, M. Mukherjee, S. Koner, Eur. J. Inorg. Chem. (2011) 2826.
[32] Bruker, APEX 2, SAINT, XPREP, Bruker AXS Inc., Madison, Wisconsin, USA, 2007.
[33] Bruker, SADABS, Bruker AXS Inc., Madison, Wisconsin, USA, 2001.
[34] SHELXS97 and SHELXL97: G.M. Sheldrick, Acta Crystallogr., Sect. A 64 (2008) 112.
[35] Y. Yang, G. Jiang, Y.-Z. Li, J. Bai, Y. Pan, X.-Z. You, Inorg. Chim. Acta (2006) 3257.
[36] J.H. Cavka, S. Jakobsen, U. Olsbye, N. Guillou, C. Lamberti, S. Bordiga, K.P. Lillerud, J. Am. Chem. Soc. 130 (2008) 13850.
[37] S. Ma, D. Yuan, X.-S. Wang, H.-C. Zhou, Inorg. Chem. 48 (2009) 2072.
[38] S. Brunauer, P.H. Emmett, E. Teller, J. Am. Chem. Soc. 60 (1938) 309.
[39] PLATON: A.L. Spek, Acta Crystallogr., Sect. D 65 (2011) 148.
[40] C. Perrio-Huard, C. Aubert, M.-C. Lasne, J. Chem. Soc., Perkin Trans. 1 (2000) 311.
[41] M. Dubey, B.G. Mishra, D. Sachdev, Appl. Catal. A 338 (2008) 20.
[42] M. Sharma, N. Agarwal, D.S. Rawat, J. Heterocycl. Chem. 45 (2008) 737.
[43] A. Yanagisawa, H. Takahashi, T. Arai, Tetrahedron 63 (2007) 8581.
[44] A. Yamaguchi, N. Aoyama, S. Matsunaga, M. Shibasaki, Org. Lett. 9 (2007) 3387.
[45] T.V. Subramanian, B. Jagannadhaswamy, G.S. Laddha, Indian J. Technol. 11 (1973) 385.
[46] G. Zhang, H. Hattori, K. Tanabe, Appl. Catal. 36 (1988) 189.
[47] J. Lopez, R. Jacquot, F. Figueras, Stud. Surf. Sci. Catal. 130 (2000) 491.
[48] R.K. Zeidan, M.E. Davis, J. Catal. 247 (2007) 379.
[49] N. Solin, L. Han, S. Che, O. Terasaki, Catal. Commun. 10 (2009) 1386.
[50] Y.M.A. Yamada, M. Shibasaki, Tetrahedron Lett. 39 (1998) 5561.